Available online at www.easletters.com

ISSN No: 2349-2864

Entomology and Applied Science Letters, 2016, 3, 4:49-56

Structure study and predict the function of the diphtheria toxin in different pH levels (Acidic-Basic-Natural) using molecular dynamics simulations

Soheila Ghaderi[1], Mohammad Reza Bozorgmehr[1,*] and Ali Morsali[1]

[1]Department of Chemistry, Mashhad Branch, Islamic Azad University, Mashhad, IRAN
Corresponding Email: bozorgmehr@mshdiau.ac.ir

ABSTRACT

Conformational switching is broadly defined as an alteration in the spatial organization of a macromolecule in response to environmental change. This study was performed to establish the relationship between variable pH and structural and functional aspect of the diphtheria toxin (DT). Molecular dynamics (MD) simulations were performed at different pH levels (4, 6.5, and 10) consist of a DT structure in water at 300K and salt concentration 0.25M at 100ns timescale simulation. Results showed that fluctuations were changed in the key residues at different pH levels. Fluctuations were more profound in the fragments A and B of DT at pH4 compared with pH6.5 and pH10. Fluctuations in the fragment A of DT (DTA) were obtained at pH4 including residues Ser9, Pro25, Tyr46, Leu73, Arg173, and Ala187. The average of the radius of gyration (Rg) and the root mean square deviation (RMSD) of the DT structure showed that decreased at pH 6.5 in comparison with pH4 and pH10. Results showed conformational changes of DT structure at pH4 compared with pH6.5 and pH10.

Keywords: Chain B of Diphtheria Toxin; Chain A of Diphtheria Toxin; Molecular dynamics simulation; Root mean square fluctuation; Variable pH;

INTRODUCTION

The historical of pH-coupled molecular dynamics are relatively short. A decade ago, Mertz and Pettitt demonstrated a titration simulation of acetic acid using an open system Hamiltonian [1].

Protein structure and function are strongly dependent on solvent pH. This dependence is due to changes in the predominant protonation state of titratable groups (chiefly side chains of certain amino acids and the termini of peptide chains) as solvent pH changes. Various structural predictions of the simulation are pH dependent molecular dynamics simulation methods which are used to predict the substrate specificity and selection of enzymes. Thereby, they provide a deep insight to studies related to structural and functional aspect [2]. Among bacterial protein toxins with an intracellular target, diphtheria toxin is one of the issues most studied. The crystal structure of DT was solved in 1992 at a resolution of 2.5 ^{o}A,[3] and was refined in 1994 at a resolution of 2.3 ^{o}A, at 2 ^{o}A using crystals of dimers of entangled monomers, [4] and finally at 1.55 ^{o}A(Steere, Weiss and Eisenberg, PDB ID 1F0L). DT is a protein of 535 amino acids organized in three structural domains of equivalent sizes, which are from the N- to the C-terminus: the catalytic (C), the transmembrane or translocation (T) and the receptor-binding (R) domains. Therefore, C corresponds to fragment A, and T and R to fragment B according to the classical denomination used for bacterial toxins with intracellular targets [5]. How the enzymatic active moiety crosses the membrane is not well-understood for any toxin but, for DT and certain other toxins (and for many animal viruses, as well), acidic intravascular pH is known to trigger the process. A variety of evidence indicates that the membrane translocation event for DT occurs when the toxin is exposed to a pH near 5.0 in the endosomal compartment [6-9]. In vitro, treatment of DT with a buffer of pH near 5.0 induces a conformational change that causes the toxin to insert into artificial lipid baitlayers [10-13], as manifested, for example, by the formation of ion-conductive membrane channels [14, 15]. Such channels have been observed both in natural and artificial membranes, but their relationship to the translocation of DTA remains uncertain [16, 17]. The fragment B of DT (DTB) mediates membrane insertion, channel formation, and translocation of DTA, and hydrophobic regions presented within DTB have been proposed to function in these

activities [18]. The pH-induced conformational switching is essential for functioning of diphtheria toxin, which undergoes a membrane insertion/translocation transition triggered by endosomal acidification as a key step of cellular entry [19].

Although the effects of pH on the conformation have been studied by various methods, there is little information available about the precise mechanism of triggering by acidic conditions [20]. As the function of these proteins resides on the stability of the 3D structure, hence, molecular dynamics simulation based analysis is essential to study the structural stability in different physiological environment [21]. The pH dependent molecular dynamics simulation methods are used to predict the substrate specificity and selection of proteins, thereby provides a deep insight into studies regarding structural and functional aspect [22].

The prime objective of this study is to evaluate the effect pH (acidic, basic, and natural) on the structure and function of the diphtheria toxin using molecular dynamic simulation. The results of the simulations of DT in different pH levels (4, 6.5, and 10) were compared by root mean square fluctuation (RMSF), Radius of gyration (Rg), Root mean square of deviation (RMSD), secondary structure and tertiary structure.

MATERIALS AND METHODS

Diphtheria toxin structure was retrieved from Protein Data Bank (PDB). The selected protein PDB ID: 1F0L was considered. The 1.55 angstrom crystal structure of wild type diphtheria toxin with X-ray diffraction was used [23]**.** It is advisable to use Deep View to preview the file if you know that your structure may be disordered. Deep View will replace any missing side chains [24]. We need to add OXT (add c-terminal oxygen) at the C-terminal end. Water molecules in the crystal were reserved in the simulations. The protonation process was done with the protein to prepare the series of protonated proteins by using H++ server, which was the input for molecular dynamics simulation [25]. The server allows quick obtaining and estimation of pKa as well as other related characteristics of bio-molecules such as isoelectric points, titration curves, and energies of protonation microstates. It also automates the process of preparing the input files for typical molecular dynamics simulations.

Protons are added to the input structure according to the calculated ionization states of the chemical groups at the user specified pH. The output structure is in the PQR (PDB + charges + radii) format. The molecular dynamics simulations were done by GROMACS 4.5.4 package by using AMBER99SB force field and periodic boundary conditions [26]. Three simulation boxes with dimensions of 9.5 × 9.5 × 9.5 nm were defined. Then, boxes were filled with the appropriate number of water molecules. In order to neutralize the system, the appropriate numbers of Na and Cl ions were added to each box. To eliminate any undesirable contacts atoms and initial kinetic energy in the simulation boxes, the energy was minimized by applying the steepest descent algorithm. The coordinates as a function of time were represented a trajectory of the system. At initial simulation (t=0) coordinates were distinguishable and were written to an output file at regular intervals. Then, each of the defining systems, was equilibrating in two stages, including 5 ns, NPT and NVT simulations with temperature and pressure fixed at 300 K and 1 bar, respectively. The pressure was controlled at 1 bar and the temperature was retained at 300K using Parrinello-Rahman Barostat [27] and V-rescale thermostat [28] respectively. For each component of the systems, PME algorithm [29] was applied to estimate the electrostatic interactions, LINCS algorithm [30] was employed to fix the chemical bonds in the atoms of the protein and was used SETTLE algorithm [31] in the solvent molecules in different pH (4,6.5,10) levels. Three simulations system were run in temperature 300K, keeping the salt concentration at 0.25M and at 100 nanoseconds. After each simulation, various properties, like RMSF, radius of gyration, RMSD, secondary structure and compact map profiles and three dimensional structures were computed and analyzed. All simulations were repeated to test the convergence of the results.

RESULTS AND DISCUSSION

We have found about fluctuations of the key to residues in the diphtheria toxin. The root mean square fluctuation (RMSF) is a measure of the deviation between the position of a particle and some reference position. The fluctuation occurs due to the protonation that influences the solvent accessibility in specific residues [32] so that, the protonation is the reason for the structural fluctuation.

Figure 1, was showed RMSF in the backbone structure of DT at different pH levels (acidic-basic –neutral). Fluctuations of the key amino acid residues in the protein structure were affected by RMSF. The solvent accessibility was dependent predominantly on buried and exposed regions of proteins, indicating the minimum and the maximum accessibility of the amino acid residues to the solvent respectively [33]. Results revealed higher fluctuations in the residues Ser9, Pro25, Tyr46, Leu73, Arg173, and Ala187 at pH4. These residues are in the C domain which is in fragment A.

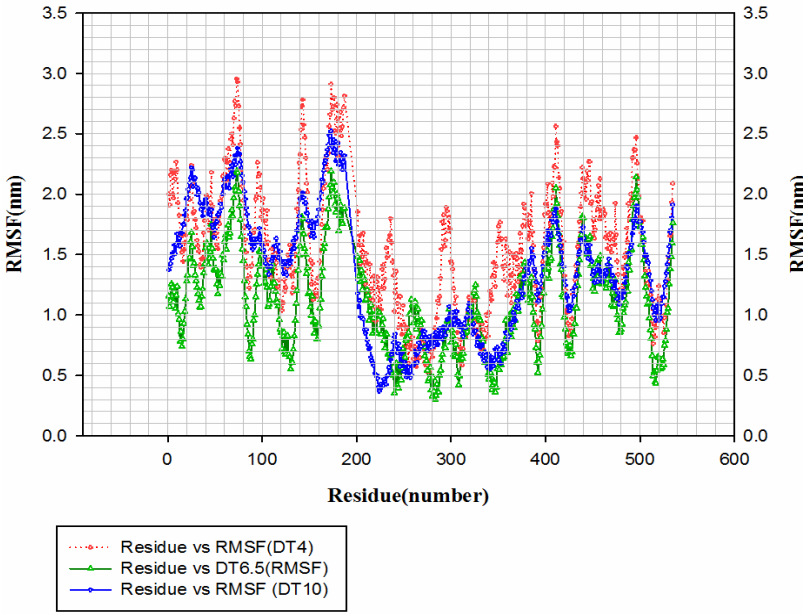

Fig. 1. Comparison of RMSF of the final DT structure, residues at 300 K in different pH levels, after 100ns timescale simulation; blue line is at pH10, red dotted line is at pH4, green line is at pH6.5

The N terminal of C domain (1–193) catalyzes the reaction of NAD+ dependent ADP ribosylation of the eukaryotic translation elongation factor eEF2 that results in protein synthesis arrest in the cell [34] and cell death via apoptosis [35].

In the previous studies and the results of the work of other scientists, the loop consists of 14 amino acid residues (186-201) linking the C domain to the T domain, which must be cleaved in order to activate DT [36-39]. Fluctuations were in the region around these residues: Lys236, Ser291, Glu292, Asp295, Glu349, Asp352, Asn373, Asn376, and Arg377 which are in T domain at pH4. T domain has 23 acidic residues, most of which are in the polar part of the sequence, this results are comparison with previous studied so that residue Glu362, which was in the middle of TH9, which residues 322-382 in the T domain (corresponding to the proposed transmembrane helices C and D) from ion channels in lipid bilayer membranes [40]. Glu349 and Asp352 are in the loop connecting helices TH8 and TH9 [41]. Also fluctuations were in the region around these residues: Lys385, and residues Glu402-Gln411 (Glu402, Asp403, Ser404, Ile405, Ile406, Arg407, Thr408, Gly409, Phe410, Gln411), Gly439, Ser446, Lys474, Ser496, Ser535, which located in R domain. These results are comparison with previous studies that at acidic pH observed residues were in R domain including Arg407–Glu413, Ala463–Thr469, and Lys516–Lys522, and from residues Ser494 to Asp507 [41]. The C-terminal of R domain (386–535) binds with a receptor on the surface of the cell [42]. These results showed fluctuations in DTA at pH4 are higher than that in DTB.

AS shown in Figure 1, at pH6.5, fluctuations were in the region around these residues: Ser535, Lys526, Ser494, Phe410, Pro378, Glu326, Thr169, Pro72 and at pH=10 fluctuations were in the region of the residues Pro25, Asn69, Gly171, Phe410, Pro438, Ser496, and Lys534. So that Arg171, Asn69, Pro25 are in DTA and other residues mention above are in DTB. Glu326 is in T domain which in region of amino acids (205–378) provides the translocation of C domain into cytosol [13].

Residues including of Ser535, Lys526, Ser494, Phe410, and Pro378 are in R domain. R has a flattened beta roll topology containing eleven strands, which roughly resemble the fold of the immunoglobulin variable domain [43]. These data are in agreement with mutagenesis studies probing the residues importance for recognition on heparin-binding epidermal growth factor-like growth factor(HB-EGF) [44, 45] and in the R domain including Lys516 and Phe530 and to a lesser extent Tyr514, Val523,Asn524, Lys526, [46] and Ser508 and Ser525 [47]. Fluctuations of T and R domains expressed by RMSF values (T domain: 1.2500nm and 1.0102nm for Glu326 and His257 respectively at pH 6.5 versus 0.8682nm and 0.4826nm at the same amino acid residues at pH 10; R domain: 1.4331nm (Pro378), 1.8759 nm (Gly409), 1.6503 nm (Lys447), 1.1521 nm (ser494) at pH 6.5 versus 1.3213nm, 1.8424nm, 1.5781nm and 1.4959nm at pH10 for the same amino acids) at pH 6.5 were higher than those at pH10. The most of the fluctuations at pH 4 were related to C domain of DTA. RMSF analyses after 100 ns timescale showed that the solvent accessibility and the amino acid residue flexibility of fragment A at pH 4 was more than those at pH 6.5 and pH 10. These results are in agreement with previous studies indicating that the low pH-induced conformational

transition of the fragment A increased binding of the protein to NAD and EF-2 [48, 49]. Comparing results of previous studies and our RMSF simulations were predicted that the lower fluctuation produces a lower binding of NAD and protein target.

The molecular spatial packing of amino acid residues is an important aspect of protein stability. A compact packing of amino acid residues is known to establish both the stability and folding rate of proteins. Radius of gyration (Rg) is a parameter that describes the equilibrium conformation of a total system, hence it provides an observation into the global dimension of protein [50]. The more compact the protein, the lower is folding rate [51]. The compactness has been defined as a ratio of the accessible surface area of a protein to the surface area of the ideal sphere of the same volume. This parameter has already been used to characterize the compactness of protein structures [52]. Rg values of diphtheria toxin were obtained from final trajectory simulations at different pHs (see Figure 2). As it has been shown, The Rg value of DT at pH 4 was 2.5150 nm at the beginning of the simulation (t=0), and it reached to 2.5288 nm at the end of the simulation (t= 100 ns). At pH 6.5, Rg was 2.5142 nm at simulation start and reached to 2.5496 nm at the end of the simulation (Figure 2). Also at pH 10, Rg was 2.5125 nm in the start of the simulation and increased to 2.5544 nm at the end of the simulation. The final trajectory files showed that average of the Rg at pH4 was more than that at pH10 and pH 6.5.

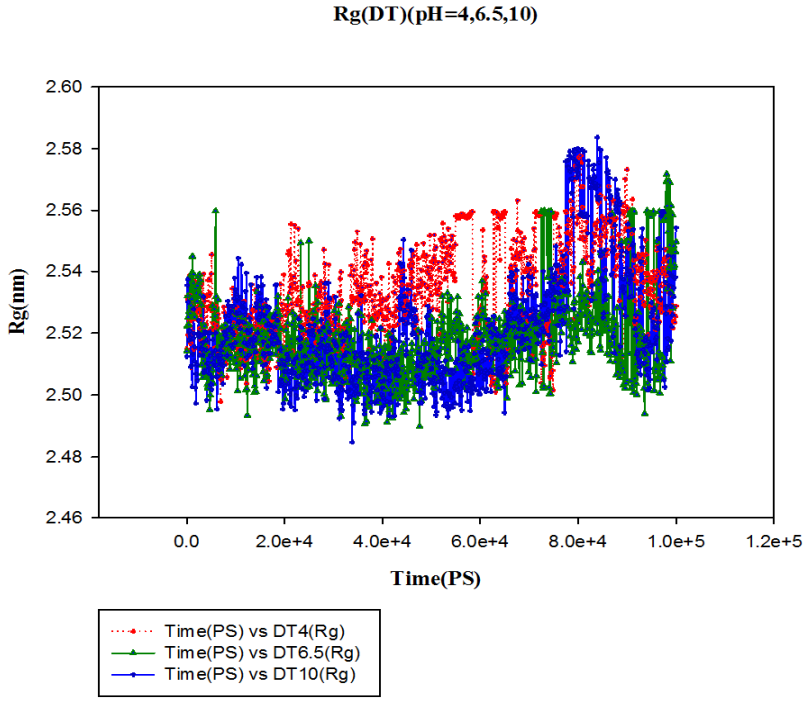

Fig. 2. Comparison of Rg of the final DT structure, residues at 300 K, in differential pH levels, after 100ns timescale simulation; blue line is at pH10, red dotted line is at pH4, green line is at pH6.5

This is justified since higher hydrophobicity would result in more compact conformations due to stronger solvent pressure [53]. From above discussions, it can be understood that the hydrophobic interaction is a main attractive force in protein folding. As results, decreased Rg can be expected increased compactness and molecular hydrophobicity of overall DT at pH6.5.

Protein folding studies often reported the root mean square deviation of the “best-predicted” structure from the crystal structure as a measure of success. All current folding procedures generated compact structures as a result of a Van der Waals’ attractive term or a hydrophobic term in their potential or pseudo-potential functions [54]. High deviations from an initial native structure can be related to the instability which is imposed by the solvent. RMSD refers to root mean square deviation from backbone of the structure to the initial starting structure [55].

The profile of RMSD was obtained from molecular dynamics simulation and has been given in the Figure 3. The overall RMSD was found to be a suitable and minimum deviation which was obtained to final structure at basic pH (pH10) with RMSD=0.1432nm and at natural pH (pH6.5) with RMSD=0.1375nm in comparison with maximum deviation (RMSD=0.1503nm) at acidic pH (pH 4). This level of fluctuation together with a minute difference in average RMSD value after the relaxation time indicate that the simulation produced stable trajectory. This is providing a suitable basis for more investigation.

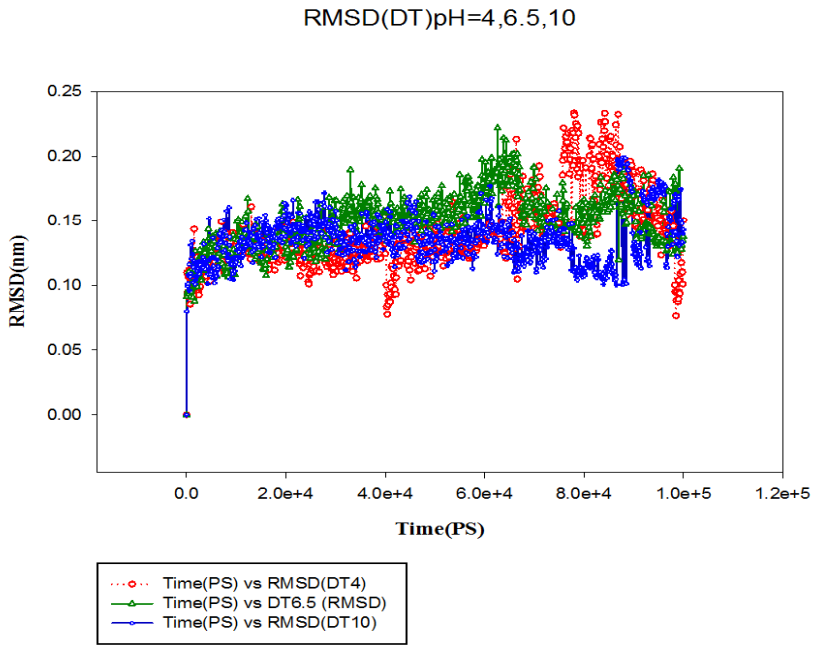

Fig. 3. RMSD of backbone atoms of the final DT structure, residues at 300 K, after 100ns timescale simulation, in differential pH levels; blue line is at pH10, red dotted line is at pH4, green line is at pH6.5

The final trajectory of DT structure after 100 ns timescale simulations at different pH levels (4, 6. 5, and 10), were analyzed with relative number of secondary structures and coils by Kabsch–Sander method [56]. As it has been shown, DT structure at pH6.5 was increased to turn and β-sheets in comparison with pH4 and pH10. In contrast, at pH6.5 coil decreased more than that of pH4 and pH10 (see table. 1). Change in β-sheets has an influence on helices and acts as a stability factor. Thereby, a significant increase of the β-sheet and turn structure has occurred in DT at neutral pH. Helix at pH4 increased more than that at pH6.5 and pH10.

Result of simulation showed that three dimensional structure of DT of the disulfide bridge (Cys186-Cys201) presented at pH6.5 and pH10 (see Figure 4(a), Figure 4(b)), however did not contain at pH4 (see Figure 4(c)). Also, hydrogen bonded was not presence between oxygen of Ala187 and hydrogen of Cys201 at pH10. In the region Tyr514-Ser525 was changed conformational structure of DT at pH4 in comparison with pH6.5 and pH10 (see Figure 5(a), Figure 5(b), Figure 5(c)). Results of three dimensional of DT structures with b-factors were shown in Figure 6 which the B-factors can be taken as indicating the relative vibrational motion of different parts of the structure.

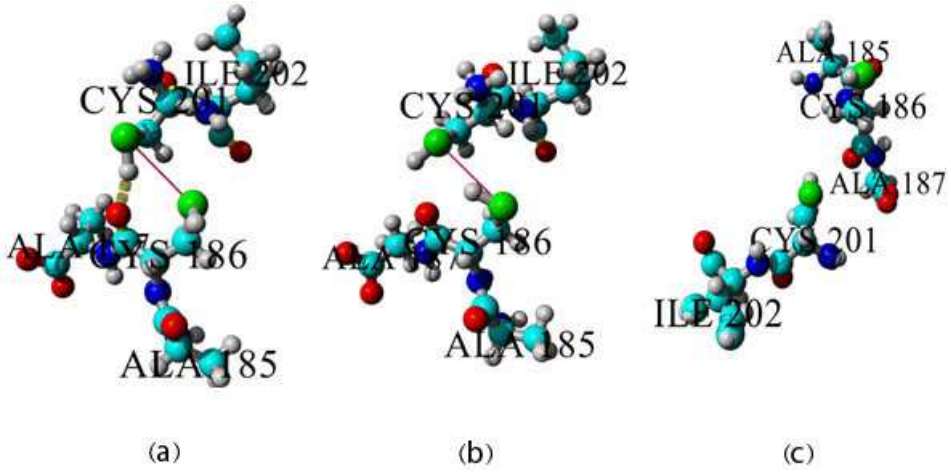

Fig. 4. Snapshots of DT structure in water at 300 K in differential pH levels in the region 185Ala-202Ile residues, after 100ns timescale simulation; a. Snapshots of DT structure in the region 185Ala-202Ile residues at pH6.5; b. Snapshots of DT structure in the region 185Ala-202Ile residues at pH10; c. Snapshots of DT structure in the region 185Ala-202Ile residues at pH4

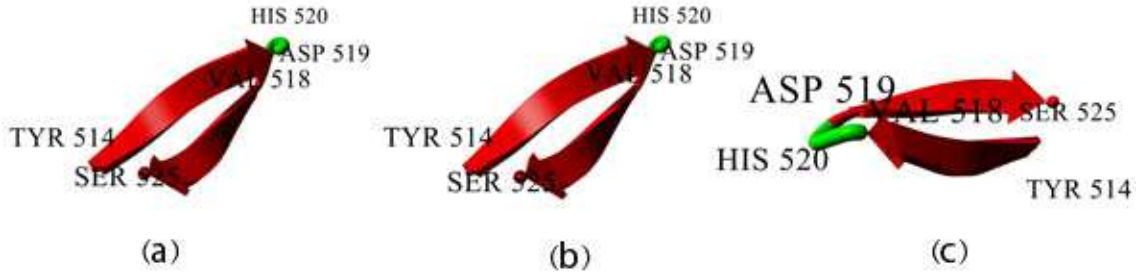

Fig. 5. Snapshots of DT structure in water at 300K in differential pH levels in the region 514Tyr-525Ser residues, after 100ns timescale simulation; a. Snapshots of the final DT structure in the region 514Tyr-525Ser residues at pH6.5; b. Snapshots of the final DT structure in the region 514Tyr-525Ser residues at pH10; c. Snapshots of the final DT structure in the region 514Tyr-525Ser residues at pH4

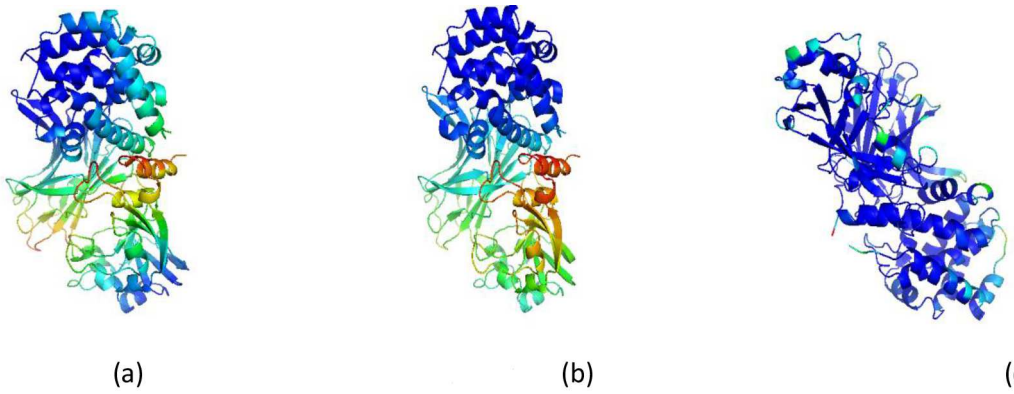

Fig. 6. Snapshots of three dimensional structure of DT at different pH levels and colored with b-factor, after 100ns timescale simulation: Blue is cool regions; Green intermediate and Red is hot (most mobile).a. Snapshots of 3 D structure of DT at pH6.5; b. Snapshots of 3 D structure of DT at pH10; c. Snapshots of 3 D structure of DT at pH4

Table 1: Comparison of secondary structure of DT at different pH levels (pH4, pH6.5 and pH10), after 100 ns simulation.

Secondary Structure	DT (pH4)	DT (pH6. 5)	DT (pH10)
Helix	30.6%	28.5%	28.5%
Sheet	28.3%	29. 2%	28.8%
Turn	11.5%	13.5%	10.8%
Coil	27.9%	25.8%	27.1%
3-10 Helix	1.7%	3.1%	4.8%

These results fully confirmed with previous studied that have been shown effect pH on the structure and function of the diphtheria toxin [19]. These results were presented detail of atom by atom in DT by molecular dynamic simulation at different pH levels.

CONCLUSION

Our results demonstrated that the conformational change of DT structure at pH 4 was more profound than that at pH 10 and pH 6.5. The conformational change was observed in the receptor binding domain (Tyr514-Ser525) and fragment A of DT. Regarding the results of molecular dynamic simulation, decreased RMSD and increased compactness of DT at pH 6.5 compared with pH 4 and pH 10. Considering our RMSF values and previous studies about the DT function at different pH values, we speculate that the more fluctuation may result in better binding of the DT structure at pH4 to NAD and the target protein in comparison with pH6.5 and pH10. These results can be used to reveal the mechanism of the DT function at different pH levels.

Acknowledgements
This work was financially supported by Department of Chemistry, Faculty of Science, Mashhad Branch, Islamic Azad University, Mashhad, Iran. We appreciate Dr. Mojtaba Noofeili of production deputy and Dr. Majid Esmaelizad of Instruments & the Central Laboratory Department, Vaccine & Serum Research Institute, Karaj, Iran.

REFERENCES

[1] Mertz JE, Pettitt BM. *International Journal of High Performance Computing Applications*. **1994**;8(1):47-53.

[2] Bürgi R, Kollman PA, van Gunsteren WF. *Proteins: Structure, Function, and Bioinformatics.* **2002**;47(4):469-80.
[3] Choe S, Bennett MJ, Fujii G, Curmi PM, Kantardjieff KA, Collier RJ, et al. The crystal structure of diphtheria toxin. **1992**.
[4] Oh KJ, Zhan H, Cui C, Hideg K, Collier RJ, Hubbell WL. *Science*. **1996**;273(5276):810-2.
[5] Menestrina G, Schiavo G, Montecucco C. *Molecular aspects of medicine*. **1994**;15(2):79-193.
[6] Draper RK, Simon MI. *The Journal of cell biology*. **1980**;87(3):849-54.
[7] Marnell MH, Shia S, Stookey M, Draper RK. *Infection and immunity.* **1984**;44(1):145-50.
[8] Middlebrook JL, Dorland RB. *Microbiological reviews*. **1984**;48(3):199.
[9] Sandvig K, Olsnes S. *The Journal of cell biology.* **1980**;87(3):828-32.
[10] Blewitt MG, Chung LA, London E. *Biochemistry*. **1985**;24(20):5458-64.
[11] Dumont M, Richards F. *Journal of Biological Chemistry*. **1988**;263(4):2087-97.
[12] Hu VW, Holmes RK. *Biochimica et Biophysica Acta (BBA)-Biomembranes.* **1987**;902(1):24-30.
[13] Sandvig K, Olsnes S. *Journal of Biological Chemistry*. **1981**;256(17):9068-76.
[14] Kagan BL, Finkelstein A, Colombini M. Diphtheria toxin fragment forms large pores in phospholipid bilayer membranes. Proceedings of the National Academy of Sciences. **1981**;78(8):4950-4.
[15] Zalman LS, Wisnieski BJ. Mechanism of insertion of diphtheria toxin: peptide entry and pore size determinations. Proceedings of the National Academy of Sciences. **1984**;81(11):3341-5.
[16] Papini E, Sandona D, Rappuoli R, Montecucco C. *The EMBO journal*. **1988**;7(11):3353.
[17] Sandvig K, Olsnes S. *Journal of Biological Chemistry.* **1988**;263(25):12352-9.
[18] Eisenberg D, Schwarz E, Komaromy M, Wall R. *Journal of molecular biology.* **1984**;179(1):125-42.
[19] Kurnikov IV, Kyrychenko A, Flores-Canales JC, Rodnin MV, Simakov N, Vargas-Uribe M, et al. *Journal of molecular biology.* **2013**;425(15):2752-64.
[20] Jiang JX, Abrams FS, London E. *Biochemistry*. **1991**;30(16):3857-64.
[21] Strom CS, Liu XY, Jia Z. *Biophysical journal.* **2005**;89(4):2618-27.
[22] James JJ, Lakshmi BS, Raviprasad V, Ananth MJ, Kangueane P, Gautam P. *Protein engineering.* **2003**; 16(12):1017-24.
[23] Steere B, Eisenberg D. *Biochemistry*. **2000**;39(51):15901-9.
[24] Guex N, Peitsch MC. *electrophoresis*. **1997**;18(15):2714-23.
[25] Hess B, Kutzner C, Van Der Spoel D, Lindahl E. *Journal of chemical theory and computation*. **2008**;4(3):435-47.
[26] Satpathy R, Guru RK, Behera R, Priyadarshini A. *J Comput Sci Syst Biol*. 2010;3(3).
[27] Parrinello M, Rahman A, Vashishta P. *Physical review letters.* **1983**;50(14):1073.
[28] Bussi G, Donadio D, Parrinello M. *The Journal of chemical physics.* **2007**;126(1):014101.
[29] Darden T, York D, Pedersen L. *The Journal of chemical physics.* **1993**;98(12):10089-92.
[30] Hess B, Bekker H, Berendsen HJ, Fraaije JG. *Journal of computational chemistry.* **1997**;18(12):1463-72.
[31] Miyamoto S, Kollman PA. *Journal of computational chemistry*. **1992**;13(8):952-62.
[32] Falconi M, Biocca S, Novelli G, Desideri A. *BMC structural biology*. **2007**;7(1):73.
[33] Gilis D, Rooman M. *Journal of molecular biology.* **1997**;272(2):276-90.
[34] Honjo T, Nishizuka Y, Hayaishi O, Kato I. *Journal of Biological Chemistry.* **1968**;243(12):3553-5.
[35] Duncan AM, Heddle JA. *Cancer letters.* **1984**;23(3):307-11.
[36] Collier R, Kandel J. Structure and Activity of Diphtheria Toxin I. *Journal of Biological Chemistry.* **1971**;246(5):1496-503.
[37] Drazin R, Kandel J, Collier R. *Journal of Biological Chemistry*. **1971**;246(5):1504-10.
[38] Gill DM, Pappenheimer A. *Journal of Biological Chemistry*. **1971**;246(5):1492-5.
[39] Gill DM, Dinius LL. *Journal of Biological Chemistry.* **1971**;246(5):1485-91.
[40] Silverman J, Mindell J, Zhan H, Finkelstein A, Collier R. *The Journal of membrane biology.* **1994**;137(1):17-28.
[41] Ghatak C, Rodnin MV, Vargas-Uribe M, McCluskey AJ, Flores-Canales JC, Kurnikova M, et al. Role of Acidic Residues in Helices TH8–TH9 in Membrane Interactions of the Diphtheria Toxin T Domain. Toxins. 2015;7(4):1303-23.
[42] Rolf JM, Gaudin HM, Eidels L. *Journal of Biological Chemistry.* **1990**;265(13):7331-7.
[43] Louie GV, Yang W, Bowman ME, Choe S. *Molecular cell.* **1997**;1(1):67-78.
[44] Mitamura T, Umata T, Nakano F, Shishido Y, Toyoda T, Itai A, et al. *Journal of Biological Chemistry.* **1997**; 272(43):27084-90.
[45] Hooper KP, Eidels L. *Biochemical and biophysical research communications.* **1996**;220(3):675-80.
[46] Shen WH, Choe S, Eisenberg D, Collier RJ. *Journal of Biological Chemistry*. **1994**;269(46):29077-84.
[47] Greenfield L, Johnson VG, Youle RJ. *Science*. **1987**;238(4826):536-9.
[48] Montecucco C, Schiavo G, Tomasi M. *Biochem J*. **1985**;231:123-8.
[49] Chung DW, Collier RJ. *Biochimica et Biophysica Acta (BBA)-Enzymology.* **1977**;483(2):248-57.

[50] Makarov DE, Keller CA, Plaxco KW, Metiu H. Proceedings of the National Academy of Sciences. **2002**;99(6):3535-9.
[51] Galzitskaya OV, Reifsnyder DC, Bogatyreva NS, Ivankov DN, Garbuzynskiy SO. *Proteins: Structure, Function, and Bioinformatics.* **2008**;70(2):329-32.
[52] Tsai C-J, Nussinov R. *Protein science: a publication of the Protein Society.* **1997**;6(7):1426.
[53] Hong L, Lei J. *Journal of Polymer Science Part B: Polymer Physics.* **2009**;47(2):207-14.
[54] Cohen FE, Sternberg MJ. *Journal of molecular biology.* **1980**;138(2):321-33.
[55] Kumar A, Purohit R. *Gene*. **2012**;511(1):125-6.
[56] Kabsch W, Sander C. *Biopolymers*. **1983**;22(12):2577-637.